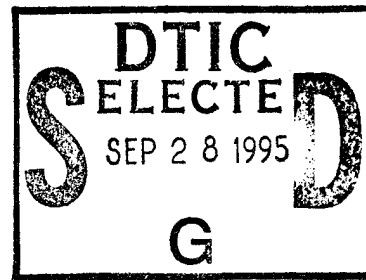


# Exposure of LDEF Materials to Atomic Oxygen: Results of EOIM-III

15 July 1995



Prepared by

M. J. MESHISHNEK, C. H. JAGGERS, and C. S. HEMMINGER  
Mechanics and Materials Technology Center  
Technology Operations

Prepared for

SPACE AND MISSILE SYSTEMS CENTER  
AIR FORCE MATERIEL COMMAND  
2430 E. El Segundo Boulevard  
Los Angeles Air Force Base, CA 90245

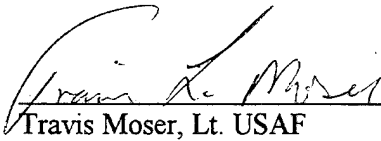
19950926 097

Engineering and Technology Group

This report was submitted by The Aerospace Corporation, El Segundo, CA 90245-4691, under Contract No. F04701-93-C-0094 with the Space and Missile Systems Center, 2430 E. El Segundo Blvd., Los Angeles Air Force Base, CA 90245. It was reviewed and approved for The Aerospace Corporation by S. Feuerstein, Principal Director, Mechanics and Materials Technology Center.

This report has been reviewed by the Public Affairs Office (PAS) and is releasable to the National Technical Information Service (NTIS). At NTIS, it will be available to the general public, including foreign nationals.

This technical report has been reviewed and is approved for publication. Publication of this report does not constitute Air Force approval of the report's findings or conclusions. It is published only for the exchange and stimulation of ideas.



---

Travis Moser, Lt. USAF  
SMC/SDES

# REPORT DOCUMENTATION PAGE

*Form Approved*  
*OMB No. 0704-0188*

Public reporting burden for this collection of information is estimated to average 1 hour per response, including the time for reviewing instructions, searching existing data sources, gathering and maintaining the data needed, and completing and reviewing the collection of information. Send comments regarding this burden estimate or any other aspect of this collection of information, including suggestions for reducing this burden to Washington Headquarters Services, Directorate for Information Operations and Reports, 1215 Jefferson Davis Highway, Suite 1204, Arlington, VA 22202-4302, and to the Office of Management and Budget, Paperwork Reduction Project (0704-0188), Washington, DC 20503.

1. AGENCY USE ONLY (Leave blank)		2. REPORT DATE <b>15 July 1995</b>	3. REPORT TYPE AND DATES COVERED	
4. TITLE AND SUBTITLE <b>Exposure of LDEF Materials to Atomic Oxygen: Results of EOIM-III</b>			5. FUNDING NUMBERS <b>F04701-93-C-0094</b>	
6. AUTHOR(S) <b>M. J. Meshishnek, C. H. Jagers, and C. S. Hemminger</b>				
7. PERFORMING ORGANIZATION NAME(S) AND ADDRESS(ES) <b>The Aerospace Corporation Technology Operations El Segundo, CA 90245-4691</b>			8. PERFORMING ORGANIZATION REPORT NUMBER <b>TR-94(4935)-12</b>	
9. SPONSORING/MONITORING AGENCY NAME(S) AND ADDRESS(ES) <b>Space and Missile Systems Center Air Force Materiel Command 2430 E. El Segundo Boulevard Los Angeles Air Force Base, CA 90245</b>			10. SPONSORING/MONITORING AGENCY REPORT NUMBER <b>SMC-TR-94-32</b>	
11. SUPPLEMENTARY NOTES				
12a. DISTRIBUTION/AVAILABILITY STATEMENT <b>Approved for public release; distribution unlimited</b>			12b. DISTRIBUTION CODE	
13. ABSTRACT ( <i>Maximum 200 words</i> )  <p>The third Effects of Oxygen Interaction with Materials (EOIM-III) experiment flew on STS-46 from July 31 to August 8, 1992. The EOIM-III sample tray was exposed to the low-earth orbit space environment for 58.55 h at an altitude of 124 nmi, resulting in a calculated total atomic oxygen (AO) fluence of <math>1.99 \times 10^{20}</math> atoms/cm<sup>2</sup>. Five samples previously flown on the Long Duration Exposure Facility (LDEF) Experiment M0003 were included on the Aerospace EOIM-III experimental tray: (1) Chemglaze A276 white thermal-control paint from the LDEF trailing edge (TE); (2) S13GLO white thermal-control paint from the LDEF TE; (3) S13GLO from the LDEF leading edge (LE) with a visible contamination layer from the LDEF mission; (4) Z306 black thermal-control paint from the LDEF TE with a contamination layer from the LDEF mission; and (5) anodized aluminum from the LDEF TE with a contamination layer from the LDEF mission. The purpose of this experiment was twofold: (1) investigate the response of trailing-edge LDEF materials to atomic-oxygen exposure, thereby simulating LDEF leading-edge phenomena; and (2) investigate the response of contaminated LDEF samples to atomic oxygen in attempts to understand LDEF contamination/atomic-oxygen interactions.</p>				
14. SUBJECT TERMS <b>LDEF, Atomic oxygen, Thermal control paints, EOIM-III</b>			15. NUMBER OF PAGES <b>32</b>	
			16. PRICE CODE	
17. SECURITY CLASSIFICATION OF REPORT <b>UNCLASSIFIED</b>	18. SECURITY CLASSIFICATION OF THIS PAGE <b>UNCLASSIFIED</b>	19. SECURITY CLASSIFICATION OF ABSTRACT <b>UNCLASSIFIED</b>	20. LIMITATION OF ABSTRACT	

## Preface

The authors wish to thank Lt. Col. Michael Obal of the Ballistic Missile Defense Organization (BMDO) for funding a portion of this work as part of the BMDO Space Environment Effects (SEE) program. We also wish to express our sincere appreciation to John Cross at Los Alamos National Laboratory for the use of his facility for the ground-based exposures. The following individuals also contributed to this work: Wayne Stuckey, Sandra Gyetvay, John Coggi, Tom Park, Dana Speece, Gloria To, and John Golden.

Accession For	
NTIS CRA&I	<input checked="" type="checkbox"/>
DTIC TAB	<input type="checkbox"/>
Unannounced	<input type="checkbox"/>
Justification .....	
By .....	
Distribution /	
Availability Codes	
Dist	Avail and/or Special
A-1	

## Contents

1.	Introduction.....	1
2.	Flight Description.....	3
3.	Sample Description and Preparation.....	5
4.	Experimental.....	7
5.	Results.....	9
	5.1 Chemglaze A276 (TE).....	9
	5.2 S13GLO (TE).....	14
	5.3 S13GLO (LE, contaminated).....	16
	5.4 Z306 (TE, contaminated).....	19
	5.5 Anodized Aluminum (TE, contaminated).....	22
6.	Comparison to Ground-Based Experiments.....	25
	6.1 Chemglaze A276 (TE).....	25
	6.2 S13GLO (TE).....	27
7.	Summary.....	29
	References.....	31

## Figures

1. Post-flight photograph of EOIM3-1-1, Chemglaze A276 LDEF TE.....	10
2. Reflectance spectra of EOIM3-1-1, Chemglaze A276 LDEF TE, before and after atomic-oxygen exposure.....	10
3. SEM photographs of EOIM3-1-1, Chemglaze A276 LDEF TE, before (left) and after (right) atomic-oxygen exposure.....	11
4. FTIR spectra of EOIM3-1-1, Chemglaze A276 LDEF TE, before and after atomic-oxygen exposure.....	12
5. Post-flight photograph of EOIM3-2-1, S13GLO LDEF TE.....	14
6. Reflectance spectra of EOIM3-2-1, S13GLO LDEF TE, before and after atomic-oxygen exposure.....	14
7. SEM photographs of EOIM3-2-1, S13GLO LDEF TE, before (left) and after (right) atomic-oxygen exposure.....	15
8. FTIR spectra of EOIM3-2-1, S13GLO LDEF TE, before and after atomic-oxygen exposure.....	16
9. Post-flight photo of EOIM3-3-1, S13GLO LDEF LE (contaminated).....	17
10. Reflectance spectra of EOIM3-3-1, S13GLO LDEF LE (contaminated), before and after atomic-oxygen exposure.....	17
11. SEM photographs of EOIM3-3-1, S13GLO LDEF LE (contaminated), before (left) and after (right) atomic-oxygen exposure.....	18
12. FTIR spectra of EOIM3-3-1, S13GLO LDEF LE (contaminated), before and after atomic-oxygen exposure.....	18
13. Post-flight photo of EOIM3-4-1, Z306 LDEF TE (contaminated).....	19
14. Reflectance spectra of EOIM3-4-1, Z306 LDEF TE (contaminated), before and after atomic-oxygen exposure.....	20
15. SEM photographs of EOIM3-4-1, Z306 LDEF TE (contaminated), before (left) and after (right) atomic-oxygen exposure.....	21
16. FTIR spectra of EOIM3-4-1, Z306 LDEF TE (contaminated), before and after atomic-oxygen exposure.....	21
17. Post-flight photo of EOIM3-5-1, anodized aluminum LDEF TE (contaminated).....	22

18. Reflectance spectra of EOIM3-5-1, anodized aluminum LDEF TE (contaminated), before and after atomic-oxygen exposure.....	22
19. FTIR spectra of EOIM3-5-1, anodized aluminum LDEF TE (contaminated), before and after atomic-oxygen exposure.....	23
20. Reflectance spectra of EOIM3-1-3, Chemglaze A276 LDEF TE, before and after atomic-oxygen exposure at LANL.....	25
21. SEM photographs of EOIM3-1-3, Chemglaze A276 LDEF TE, before (left) and after (right) atomic-oxygen exposure at LANL.....	26
22. Reflectance spectra of EOIM3-2-3, S13GLO LDEF TE, before and after atomic-oxygen exposure at LANL.....	27
23. SEM photographs of EOIM3-2-3, S13GLO LDEF TE, before (left) and after (right) atomic-oxygen exposure at LANL.....	27

### Tables

1. Weights of EOIM-III Samples.....	9
2. Solar Absorptance Calculations of EOIM-III Samples.....	11
3. XPS Surface Analysis of EOIM-III Flight Samples .....	13

## 1. Introduction

Specimens retrieved from the Long Duration Exposure Facility (LDEF) showed dramatic differences between the response of materials located on the leading edge (LE) and those on the trailing edge (TE). These differences are largely attributed to the high fluence of atomic oxygen to which the leading-edge specimens were exposed.<sup>1</sup> The synergistic effects between UV radiation and atomic oxygen have also received much attention since the return of LDEF. Typical responses of white thermal-control paints on the trailing edge included darkening due to the UV exposure. However, paint specimens on the leading edge of LDEF in many cases retained their white properties, presumably due to the scrubbing effects of atomic oxygen, which removed the UV damaged layer.<sup>1-3</sup> Contamination on LDEF has, and continues to be, actively investigated, especially with respect to reaction with UV and atomic oxygen.<sup>4-8</sup>

The purpose of this experiment was twofold. First, we wished to simulate LDEF LE phenomena by exposing TE samples of white paints to low Earth orbit atomic oxygen. Second, we wanted to see if contamination layers on TE specimens could be removed and/or chemically altered by the atomic-oxygen exposure. The exposure of these materials on EOIM-III can be compared to recent results obtained from ground-based, atomic-oxygen exposures using O-atom facilities at Los Alamos National Laboratory (LANL).

## 2. Flight Description

The third Effects of Oxygen Interaction with Materials (EOIM-III) experiment flew on STS-46 from July 31 to August 8, 1992. The EOIM-III sample tray was exposed to the low Earth orbit space environment for 58.55 h at an altitude of 124 nmi. The sample tray was exposed to a calculated total atomic-oxygen (AO) fluence of  $1.99 \times 10^{20}$  atoms/cm<sup>2</sup>. Five samples previously flown on the M0003 LDEF experiment were included on the Aerospace experimental tray: (1) Chemglaze A276 white thermal control paint from the LDEF trailing edge (TE); (2) S13GLO white thermal control paint from the LDEF TE; (3) S13GLO from the LDEF leading edge (LE) with a visible contamination layer from the LDEF mission; (4) Z306 black thermal control paint from the LDEF TE with a contamination layer; and (5) anodized aluminum from the LDEF TE with a contamination layer.

### 3. Sample Description and Preparation

Chemglaze A276 is a white thermal control paint manufactured by Lord Corporation that consists of primarily a titanium dioxide pigment in a polyurethane binder. This paint was used on LDEF as a thermal control coating on the Experiment Power and Data System (EPDS) sunshields. The samples used for EOIM-III were sectioned from The Aerospace Corporation LDEF experiment EPDS sunshield located on the LDEF trailing edge at D4.<sup>1</sup> The sunshield exposure was 10,400 equivalent sun hours of UV radiation and an atomic-oxygen fluence of  $2.31 \times 10^5$  atoms/cm<sup>2</sup> during the LDEF mission.<sup>9,10</sup> Unlike leading-edge samples of Chemglaze A276, these samples did not show evidence of atomic oxygen erosion from the LDEF mission due to their exposure to a much lower atomic oxygen fluence (by about 17 orders of magnitude).<sup>1,3</sup> The samples rather had been considerably darkened from UV radiation but remained quite glossy and specular.

S13GLO is a white thermal control paint manufactured by IITRI that incorporates a zinc oxide pigment in a methyl silicone binder. The ZnO pigment is encapsulated with potassium silicate for increased radiation stability. The samples were sectioned from the leading- and trailing-edge signal conditioning unit (SCU) covers on trays D8 and D4, respectively.<sup>1</sup> The LE samples had previously been exposed to 9400 equivalent sun hours of UV radiation and an atomic oxygen fluence of  $8.99 \times 10^{21}$  atoms/cm<sup>2</sup>.<sup>9,10</sup> The LE samples used for the EOIM-III experiment were contaminated with a dark-brown/tan contamination layer, which significantly increased the paint's solar absorptance. However, the samples were taken from the side of the SCU cover so they saw no direct exposure to atomic oxygen, but may have seen some reflected or scattered AO during the LDEF mission. The contamination was the result of venting of contamination from the interior of LDEF.

The TE S13GLO samples used for the EOIM-III experiment, like the Chemglaze A276 TE samples, were exposed to 10,400 equivalent sun hours of UV radiation and an atomic oxygen fluence of  $2.31 \times 10^5$  atoms/cm<sup>2</sup>.<sup>9,10</sup> These samples had also been significantly darkened by the UV exposure.<sup>1</sup> There was no significant contamination layer on these samples, as was the case for the LE specimens.

Chemglaze Z306 is a black thermal control paint manufactured by Lord Corporation that incorporates a carbon-black pigment in a polyurethane binder. Samples were sectioned from a module backing plate on the LDEF trailing edge tray at location D3. This painted surface was facing inside of LDEF and, therefore, was not subjected to UV radiation or atomic oxygen impingement. The backing plate did, however, have a visible contamination layer from the outgassing of various components and/or experiments on LDEF.

Anodized aluminum samples were sectioned from the environmental exposure control canister (EECC) located on the LDEF trailing edge at D4. Consequently, it had been exposed to 10,400 equivalent sun hours of UV radiation and an atomic oxygen fluence of  $2.31 \times 10^5$  atoms/cm<sup>2</sup>.<sup>9,10</sup> A light-brown contamination layer was present on the surface due to the outgassing of various components and/or experiments on LDEF and their subsequent photo-fixing from the UV exposure.<sup>1</sup>

The samples were sectioned into several 1-in.-diam discs. The following sample notation and descriptions were used for identification purposes:

EOIM3-X-Y

where X = Material Designation as follows:

- 1 = Chemglaze A276 white thermal control paint on aluminum substrate from trailing edge of LDEF (D4 sunshield)
- 2 = S13GLO white thermal control paint on aluminum substrate from trailing edge of LDEF (D4 signal conditioning unit cover)
- 3 = S13GLO white thermal control paint on aluminum substrate from leading edge of LDEF with contamination stain (D8 signal conditioning unit cover)
- 4 = Z306 black thermal control paint on aluminum substrate from trailing edge of LDEF with contamination stain (Interior module backing plate from tray D3)
- 5 = Aluminum section from trailing edge of LDEF with contamination stain (D4 EECC sunshield)

Y = Sample use designation as follows:

- 1 = Flight sample
- 2 = Control Sample
- 3-5 = LANL, Analysis samples

All samples were baked for at least 24 h at a minimum temperature of 65°C and a maximum pressure of  $2 \times 10^{-6}$  torr to meet EOIM-III flight contamination requirements.

## 4. Experimental

The flight samples were characterized before and after the EOIM-III mission and compared to the control samples. Sample weight, solar absorptance, surface analysis, and surface morphology were all determined for each sample by the methods described below.

Changes in the optical properties of thermal control materials, especially solar absorptance, is the primary indication of degradation after exposure to the space environment. Diffuse reflectance spectra of the samples from 250–2500 nm were obtained using a Perkin-Elmer Lambda 9 UV/VIS/NIR spectrophotometer equipped with a barium sulfate integrating sphere. Solar absorptance values for each sample were calculated from the spectra after normalization to a NIST diffuse-reflectance standard. The precision of the measurement is  $\pm 0.003$ ; however, absorption of the material outside the range of measurement can produce errors in accuracy of 4%.

X-ray Photoelectron Spectroscopy (XPS) was used to investigate the surface chemistry of the samples and to detect any surface compositional changes. A VG Scientific ESCALAB MK II multiprobe instrument was used for the XPS analyses. The samples were mounted on sample stubs with double-sided tape. Survey scans from 0 to 1100 eV binding energy were acquired with a Mg  $K\alpha$  source to qualitatively determine the sample surface composition. Analysis areas were about  $4 \times 5$  mm in size and to a depth of 50–100 Å. High-resolution elemental scans were subsequently run to obtain semi-quantitative elemental analyses from peak area measurements and chemical state information from the details of binding energy and shape. Measured peak areas for all detected elements were corrected by elemental sensitivity factors before normalization to give surface mole %. The quantization error on a relative basis is  $\leq 10\%$  of the measurement for components with a surface concentration  $> 1$  mole %. Large uncertainties in the relative elemental sensitivity factors can introduce absolute errors of a factor of 2 or even greater. The detection limit is about 0.1 surface mole %, but spectral overlaps between large and small peaks can make it impossible to detect minor components, particularly when more than one chemical state is present for a given element.<sup>11</sup>

Changes in surface composition and structure were also investigated using Fourier-Transform Infrared Spectroscopy (FTIR). FTIR spectra were obtained by the diffuse reflectance method using a Nicolet MX-1 infrared spectrometer scanning from 4000 to 400  $\text{cm}^{-1}$ .

The surface morphologies of the control and flight samples were compared using a JEOL JSM-840 Scanning Electron Microscope (SEM). An accelerating voltage of 15 keV was used for all sample observations. Photographs of the samples were taken at magnifications from 100–5000 $\times$ . It was necessary to carbon-coat the paint samples prior to analyses to eliminate the surface charging effects that distorted the SEM images.

## 5. Results

Optical and surface analysis measurements were performed on all of the flight and control samples, both before and after the EOIM-III mission. However, due to the destructive nature of the SEM investigations (i.e., carbon-coating the samples), no preflight SEM analyses were performed on the flight samples. Thus, comparisons were made between post-flight and control samples.

Pre- and post-flight weight measurements of the samples are listed in Table 1. Quantitative conclusions from these measurements are difficult since there was some contamination of many samples during the EOIM-III mission. However, the measurements are qualitatively consistent with the other results, as discussed below. The net weight gain for the S13GLO samples is unusual and may be due to re-absorption of water vapor postflight.

Table 1. Weights of EOIM-III Samples

Sample	Sample ID	Weight (g)		
		Pre-flight	Post-flight	Change
Chemglaze A276	EOIM3-1-1	1.394380	1.394300	-0.000080
S13GLO TE	EOIM3-2-1	1.323910	1.324040	+0.000130
S13GLO LE	EOIM3-3-1	1.300280	1.300810	+0.000530
Chemglaze Z306	EOIM3-4-1	2.191500	2.191410	-0.000090
Aluminum	EOIM3-5-1	2.241205	2.241180	-0.000025

### 5.1 Chemglaze A276 (TE)

The trailing-edge LDEF sample (EOIM3-1-1) of Chemglaze A276 showed marked changes due to the EOIM-III exposure, as expected. Visual inspection revealed that the sample changed from brown to white during the experiment, and the surface became more diffuse. A photograph of the post-flight sample is shown in Figure 1. The UV-VIS-NIR spectra (Figure 2) show increased reflectance after the exposure and that the change in the material primarily occurred in the visible-wavelength range. The solar absorptance decreased from 0.528 to 0.295 (Table 2).

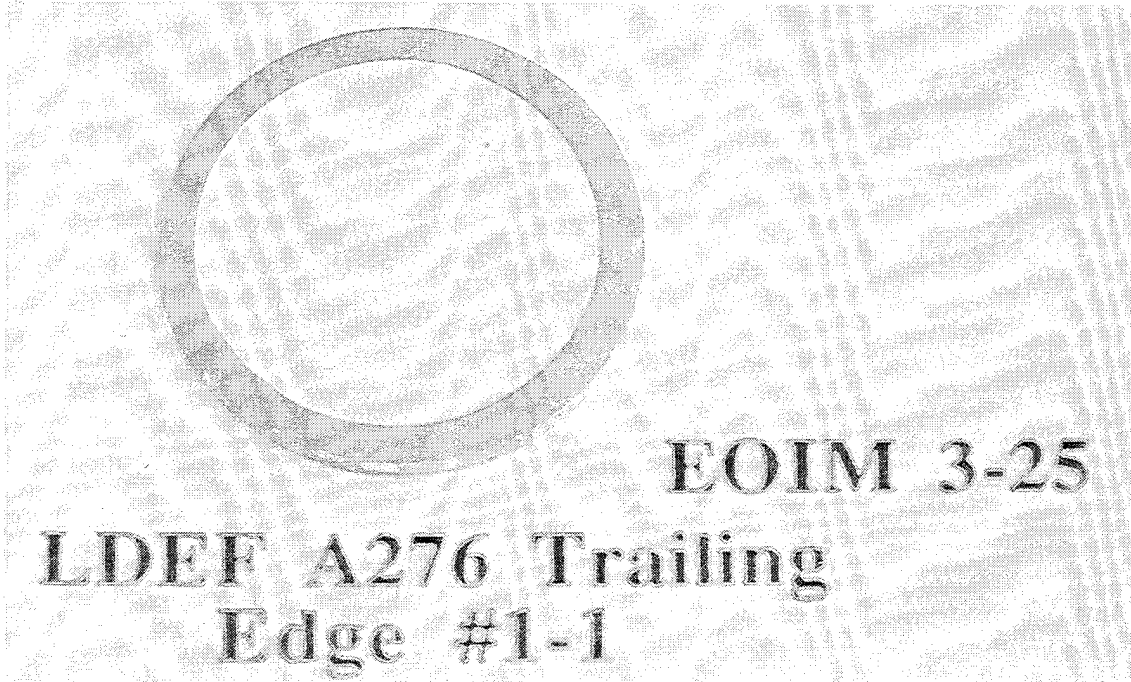


Figure 1. Post-flight photograph of EOIM3-1-1, Chemglaze A276 LDEF TE.

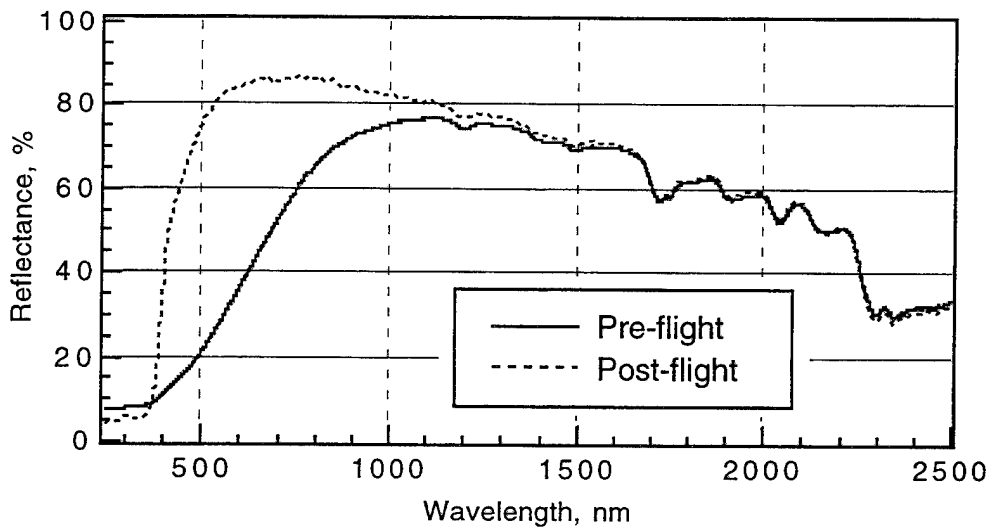


Figure 2. Reflectance spectra of EOIM3-1-1, Chemglaze A276 LDEF TE, before and after atomic-oxygen exposure.

Table 2. Solar Absorptance Calculations of EOIM-III Samples

Sample	Sample ID	Type	Solar Absorptance		
			Pre-flight	Post-flight	Change
Chemglaze A276	EOIM3-1-1	Flight	0.528	0.295	-0.233
	EOIM3-1-2	Control	0.537	0.534	-0.003
	EOIM3-1-3	LANL	0.536	0.258	-0.278
S13GLO	EOIM3-2-1	Flight	0.417	0.355	-0.062
	EOIM3-2-2	Control	0.424	0.422	-0.002
	EOIM3-2-3	LANL	0.422	0.386	-0.036
S13GLO	EOIM3-3-1	Flight	0.507	0.515	+0.008
	EOIM3-3-2	Control	0.515	0.506	-0.009
Chemglaze Z306	EOIM3-4-1	Flight	0.955	0.960	+0.005
	EOIM3-4-2	Control	0.953	0.952	-0.001
Aluminum	EOIM3-5-1	Flight	0.394	0.330	-0.064
	EOIM3-5-2	Control	0.393	0.390	-0.003

Investigation of the surface morphology by SEM (Figure 3) indicates the expected changes due to the atomic oxygen exposure. The flight sample, in comparison to the ground control, indicates a significant roughening of the surface from erosion. The control sample, which has not been exposed to significant amounts of atomic oxygen, appears to be relatively intact with the titanium dioxide pigment particles dispersed throughout the polyurethane binder. However, the polyurethane binder on the surface of the flight sample was eroded away, leaving a surface that is primarily titanium dioxide pigment. These differences were also seen between LDEF leading- and trailing-edge samples.<sup>1,3</sup>

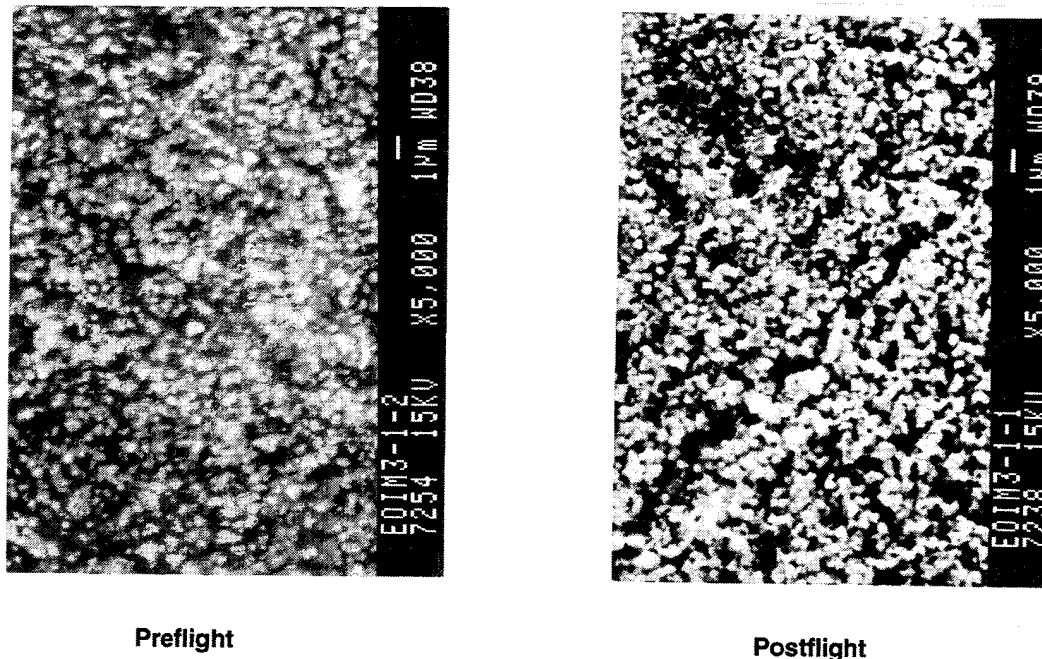


Figure 3. SEM photographs of EOIM3-1-1, Chemglaze A276 LDEF TE, before (left) and after (right) atomic oxygen exposure.

The preflight and postflight FTIR spectra of the Chemglaze A276 sample are shown in Figure 4. There is an apparent reduction in infrared absorption throughout the wavelength range, suggesting a thinning of the polyurethane binder layer from atomic-oxygen erosion. This is consistent with the SEM observations. However, no significant spectral shifts or intensity-ratio changes were observed, suggesting uniform erosion of the polyurethane. There appears to be a small change in the absorption ratio at  $750\text{ cm}^{-1}$ , which may be due to removal of aromatic hydrogens in the polyurethane.

The XPS results for the Chemglaze A276 sample (Table 3) indicate changes to the surface chemical composition.<sup>12</sup> The preflight surface silicon is presumably due to contamination. An increase of 6.5 atom % of surface silicon was detected on the post-flight sample, which is attributed to flight contamination and uncovering of an aluminum silicate filler/extender (used in the Chemglaze paints) as the binder erodes away.<sup>2</sup> The corresponding increase in aluminum is consistent with this hypothesis. The 40% decrease in carbon concentration is explained by loss of surface carbon contamination and polyurethane binder by reaction with atomic oxygen. The increase in surface oxygen could be due to deposition of silicone contaminants during the EOIM-III mission, exposure of the aluminum silicate, or oxidation of surface silicones. The predominant chemical state of silicon on all Chemglaze A276 samples appeared to be silica,  $\text{SiO}_2$ , based on a  $\text{Si}2p$  binding energy close to 103.5 eV after charge correction. Silica is thought to be a degradation product of Silicone contaminants upon atomic oxygen exposure and for UV radiation damage. Other samples on the Aerospace EOIM-III tray had postflight increases in surface silicon that had to have been caused by flight contamination.<sup>12</sup> The small increase in titanium signal and decrease in nitrogen concentration are also consistent with loss of surface binder. Pre-flight contamination is presumed to be responsible for the surface tin signal.

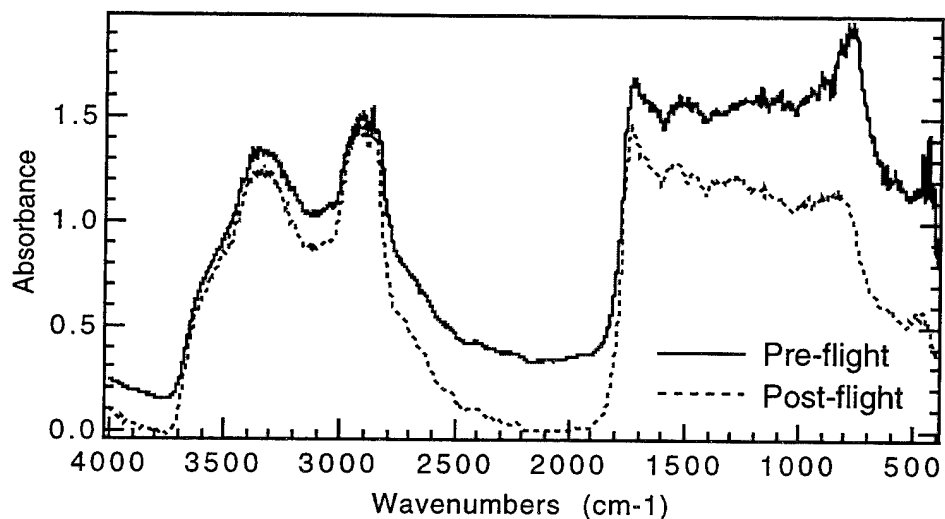


Figure 4. FTIR spectra of EOIM3-1-1, Chemglaze A276 LDEF TE, before and after atomic-oxygen exposure.

Table 3. XPS Surface Analysis of EOIM-III Flight Samples

Sample	Surface Mole % (Normalized)										
	C	O	Si	Sn	Ti	N	S	Cl	Na	F	Al
Chemglaze A276 (TE):											
EOIM3-1-1											
Pre-flight	51	38	5.5	0.7	trace	3.1	0.4	0.2	0.5	0.6	~0.2
Post-flight	30	51	12	1.1	0.4	2.7	0.2	trace	1.7	0.4	~3
EOIM3-1-3 (LANL)											
Pre-exposure	50	38	7.5	0.5	trace	2.9	0.4	0.1	0.4	0.4	~0.2
Post-exposure	23	52	14	1.2	0.6	1.2	0.5	nd	1.6	0.2	6.1
Z306 (TE, contaminated):											
EOIM3-4-1											
Pre-flight	30	53	15	0.1	nd	1.4	0.2	nd	0.1	0.3	
Post-flight	23	56	19	0.1	nd	1.1	trace	nd	trace	0.2	

Sample	Surface Mole % (Normalized)									
	C	O	Si	K	Zn	N	S	Cl	Na	F
S13GLO (TE):										
EOIM3-2-1										
Pre-flight	33	43	19	0.6	0.3	2.2	0.5	0.4	0.5	0.4
Post-flight	22	47	25	0.8	1.8	2.2	0.1	1.1	0.4	0.1
EOIM3-2-3 (LANL)										
Pre-exposure	34	41	21	0.6	0.4	1.9	0.6	0.4	0.3	0.2
Post-exposure	21	49	28	0.2	0.3	0.7	0.3	0.2	0.1	nd
S13GLO (LE, contaminated):										
EOIM3-3-1										
Pre-flight	19	53	28	nd	nd	0.2	0.2	nd	nd	nd
Post-flight	16	55	29	nd	trace	0.2	trace	trace	nd	0.1

Sample	Surface Mole % (Normalized)											
	C	O	Si	Al	Sn	K	Ca	N	S	Cl	Na	F
Anodized Aluminum (TE, contaminated):												
EOIM 3-5-1												
Pre-flight	46	37	5.7	4.8	0.4	0.3	0.3	1.7	0.3	0.2	2.4	0.4
Post-flight	11	57	11	14	0.5	0.8	0.2	0.5	0.6	0.3	2.3	2

The sample weight of the Chemglaze A276 sample (Table 1) shows a net decrease, which is consistent with the observation that atomic oxygen erosion caused removal of the polyurethane binder.

## 5.2 S13GLO (TE)

The S13GLO sample from the trailing edge of LDEF visually appeared whiter in comparison to the control sample and to the masked region of the flight sample (Figure 5). The sample exhibited increased post-flight reflectance in the visible wavelength range (Figure 6), resulting in a decreased solar absorptance from 0.417 to 0.355 (Table 1).

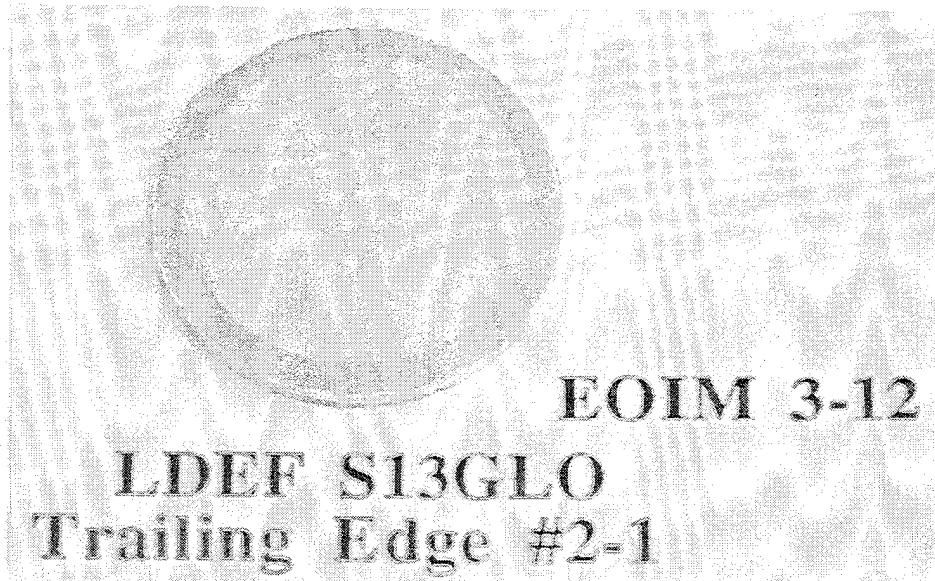


Figure 5. Post-flight photograph of EOIM3-2-1, S13GLO LDEF TE

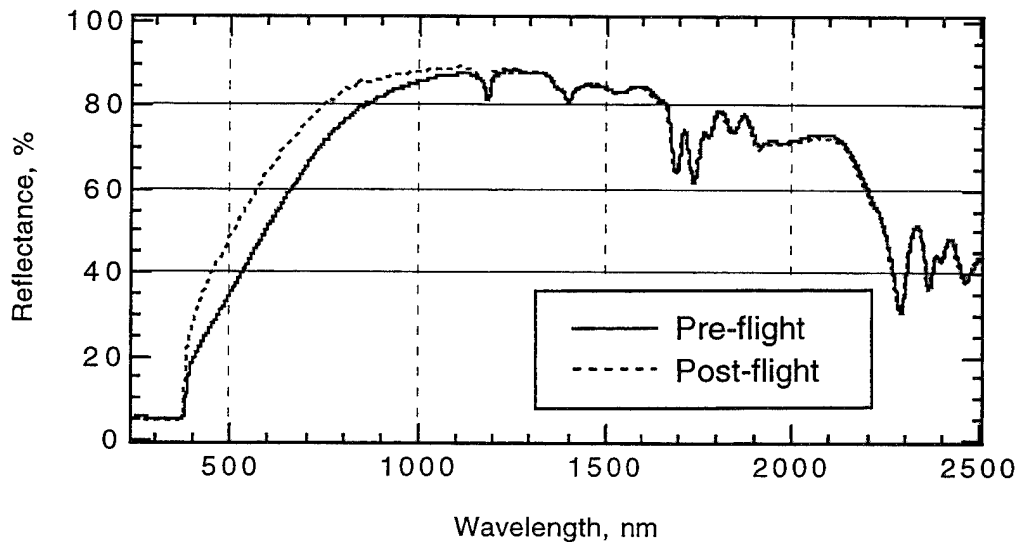


Figure 6. Reflectance spectra of EOIM3-2-1, S13GLO LDEF TE, before and after atomic oxygen exposure.

Investigation of the surface morphology with SEM (Figure 7) indicates that exposure to atomic oxygen resulted in minor changes. The surface of the flight sample appears to have been slightly eroded by atomic oxygen, although not as extensively as the Chemglaze A276 sample. As with Chemglaze A276, the erosion was probably due to atomic oxygen erosion of the binder. However, in this case, erosion of the silicone is much less than the polyurethane used in the Chemglaze paints. Erosion of the S13GLO binder was not observed on M0003 LDEF samples.<sup>1,3</sup>

Figure 8 gives the pre-flight and post-flight FTIR spectra for the TE S13GLO sample. Some decreased absorbance is noted for the sample after the exposure. There is a significant but small decrease in the absorption at  $3000\text{ cm}^{-1}$  due to the C-H stretch, indicating oxidative removal of the methyl groups attached to the silicone polymer. This effect has been observed on earlier EOIM flights.<sup>13</sup>

XPS post-flight analysis showed a significant decrease in the surface carbon concentration, an increase in the surface silicon concentration, and a small increase in the surface oxidation relative to the pre-flight analysis (Table 3).<sup>12</sup> The increase in silicon concentration is probably due to contaminant deposition, although it is impossible to distinguish between the possible sources of silicon (contaminant silicones, methyl silicone binder, potassium silicate encapsulate). The charge-corrected binding energy of the Si2p peak shifted by about half a volt (from 103.2 eV to 103.8 eV) between pre- and post-exposure analyses for the S13GLO samples exposed to atomic oxygen. This indicates that silica was the predominant state on all surfaces, but some additional oxidation of residual surface Silicones or silicates probably took place during the atomic oxygen exposures. The increase in potassium and larger increase in zinc signal indicates that some loss of surface binder occurred.

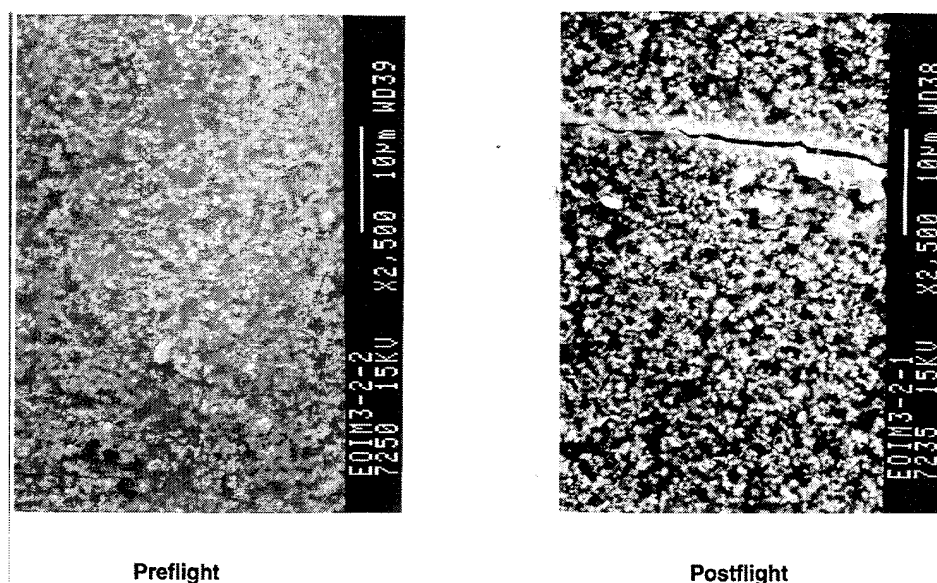


Figure 7. SEM photographs of EOIM3-2-1, S13GLO LDEF TE, before (left) and after (right) atomic oxygen exposure.

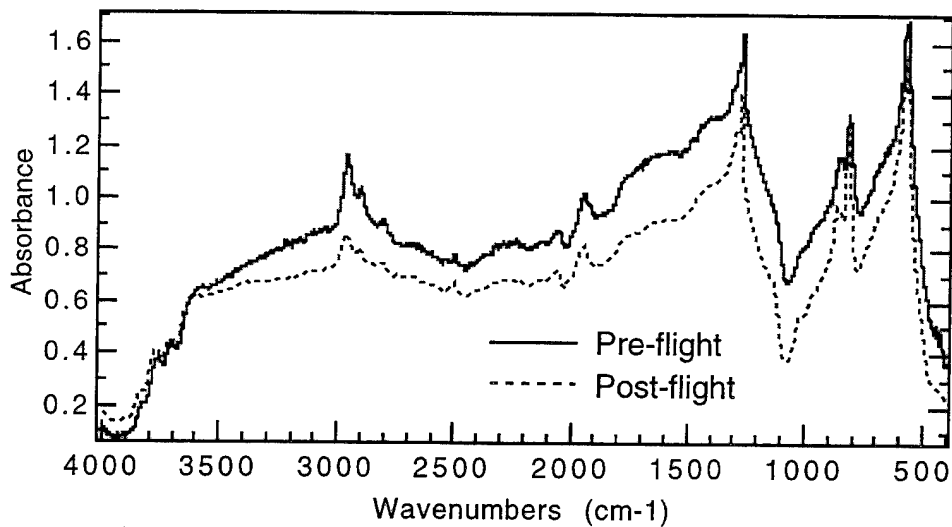


Figure 8. FTIR spectra of EOIM3-2-1, S13GLO LDEF TE, before and after atomic oxygen exposure.

The sample weight (Table 1) increased slightly during the EOIM-III experiment. However, it did not increase as much as for the S13GLO (LE, contaminated) sample, which was relatively inert to atomic oxygen exposure (see next section). These facts are consistent with the hypothesis that atomic oxygen erosion of the methyl silicone binder did occur, but the total weight loss was slightly less than the weight gain due to flight contamination or re-absorbed water vapor.

### 5.3 S13GLO (LE, contaminated)

The S13GLO sample from the side of the SCU cover on the leading edge of LDEF was recovered still visibly contaminated with a brown "nicotine" stain. The post-flight photo of this sample is shown in Figure 9. The reflectance spectra in Figure 10 indicate very little change resulting from atomic oxygen exposure; the solar absorptance increased insignificantly from 0.507 to 0.515 (Table 2).



Figure 9. Post-flight photo of EOIM3-3-1, S13GLO LDEF LE (contaminated).

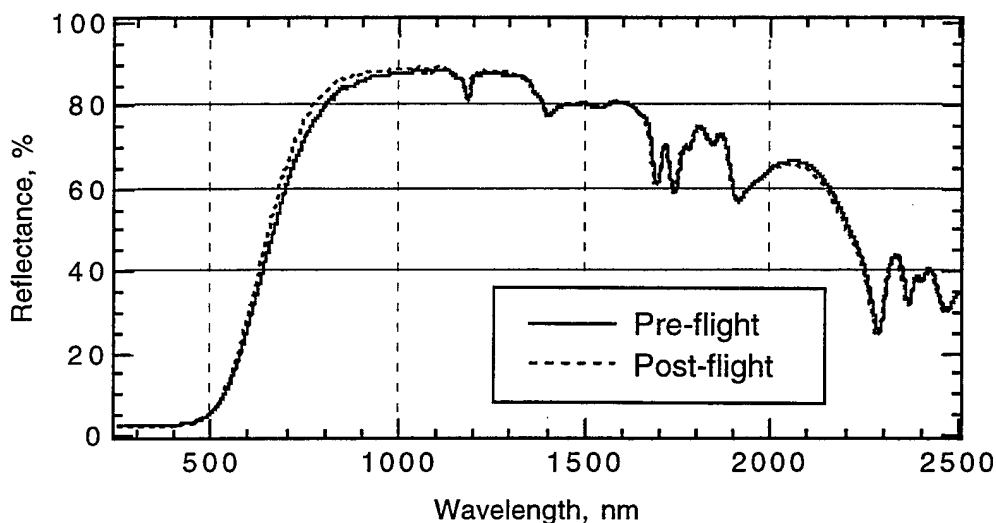


Figure 10. Reflectance spectra of EOIM3-3-1, S13GLO LDEF LE (contaminated), before and after atomic oxygen exposure.

The SEM photographs in Figure 11 show a significantly different surface morphology than the S13GLO LDEF TE sample, presumably due to the contamination layer. From the SEM photographs, it appears that the contamination layer grows from nucleation sites on the surface in an upward direction, away from the surface. Both the flight sample (after atomic oxygen exposure) and the control sample (no atomic oxygen exposure) have similar surface morphologies, indicating that atomic oxygen had little effect on this contamination layer.

The FTIR spectra for the LE S13GLO sample are given in Figure 12. Essentially no changes occurred due to the atomic oxygen exposure. Overall absorption changes are evident due to thickness differences in different areas of the paint sample.

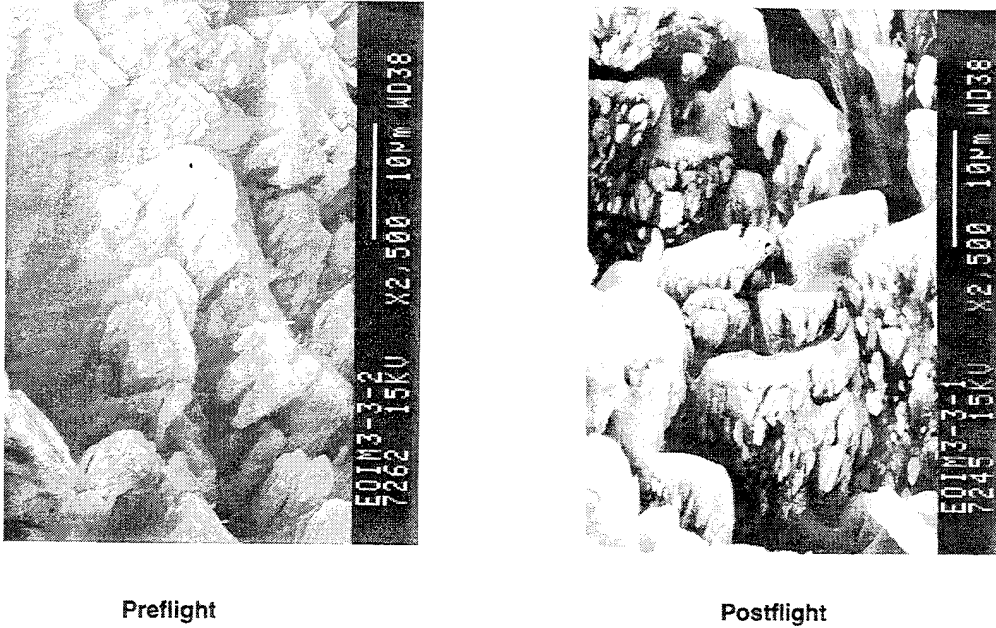


Figure 11. SEM photographs of EOIM3-3-1, S13GLO LDEF LE (contaminated), before (left) and after (right) atomic oxygen exposure.

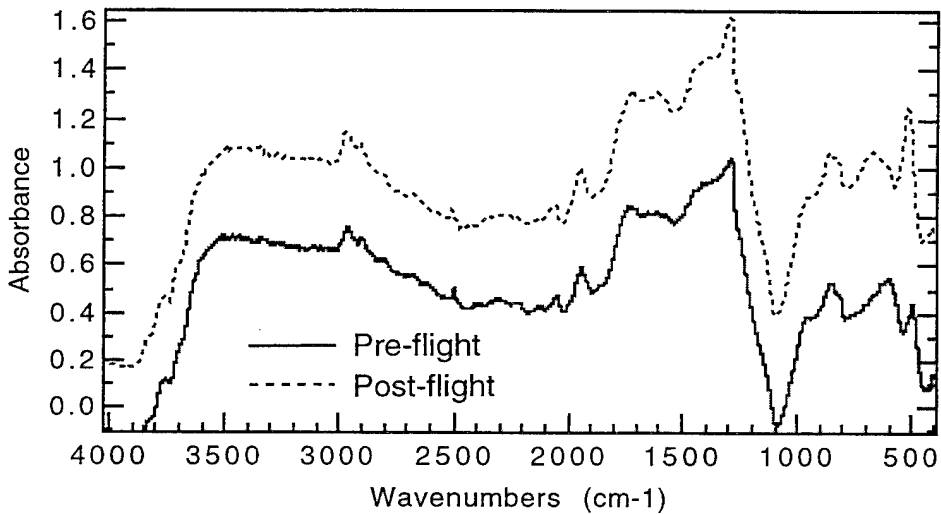


Figure 12. FTIR spectra of EOIM3-3-1, S13GLO LDEF LE (contaminated), before and after atomic oxygen exposure.

Post-flight XPS analysis of the sample showed very little significant change in the surface composition (Table 3).<sup>12</sup> A small decrease in the surface carbon concentration was noted. The contamination layer from the LDEF exposure appears to be quite stable to further atomic oxygen exposure. The binding energy of the Si2p peak indicates that the predominant surface state is silica, which is consistent with its stability to the space environment.

The sample weight increased after the EOIM-III exposure (Table 1). The sample analyses show that this sample was relatively inert to atomic oxygen, thus causes for the apparent weight gain are unknown. However, it may be unique to the material S13GLO since both EOIM-III samples gained weight. Reabsorbed water is a possible source.

#### **5.4 Z306 (TE, contaminated)**

The sample of Z306 from the trailing edge of LDEF flown on EOIM-III exhibited only a slight change in its reflectance post-flight, resulting in a negligible increase in its solar absorptance from 0.955 to 0.960 (Table 2). Visually the sample appeared the same as before the flight (Figure 13). The reflectance spectra are shown in Figure 14. However, XPS and SEM results indicate that significant changes did occur due to atomic oxygen erosion.

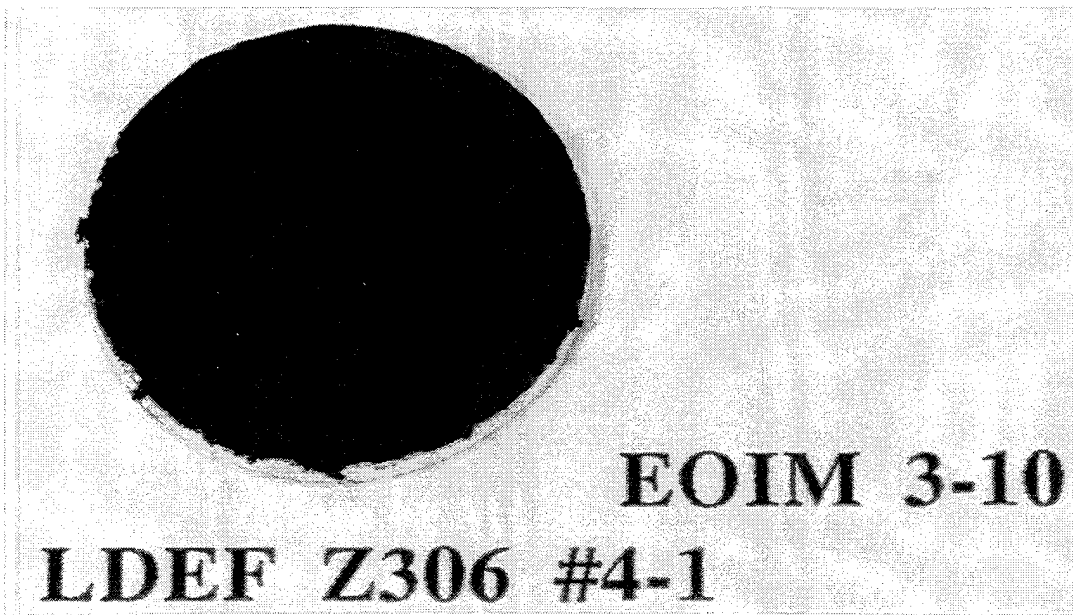


Figure 13. Post-flight photo of EOIM3-4-1, Z306 LDEF TE (contaminated).

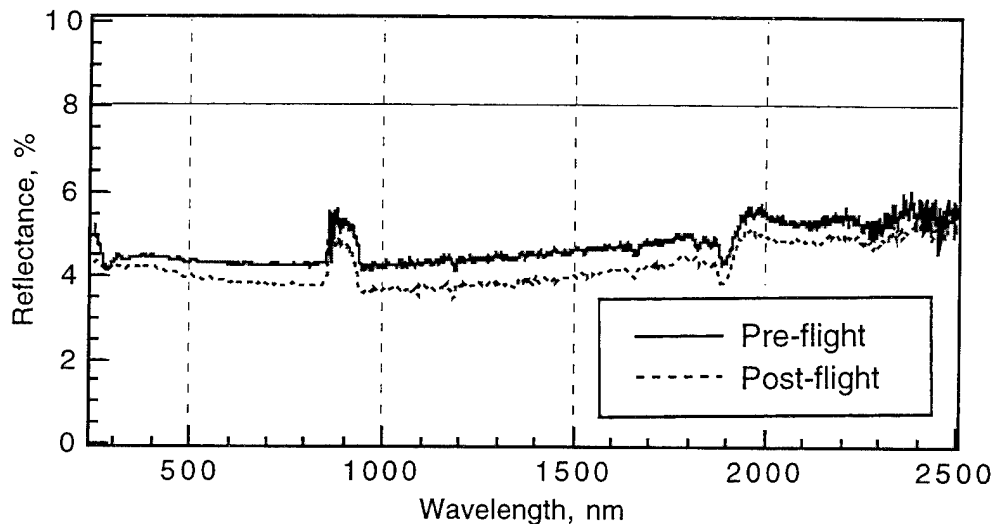


Figure 14. Reflectance spectra of EOIM3-4-1, Z306 LDEF TE (contaminated), before and after atomic oxygen exposure.

The XPS data in Table 3 show a significant loss of surface carbon, which may be due to a loss of either carbon-black pigment and/or polyurethane binder. A decrease of surface nitrogen concentration indicates a minor loss of surface binder. The large preflight surface silicon is due to the contamination layer on the sample. The increase in silicon may be due to flight contamination or the exposure of a silicate filler due to erosion of the binder.

The surface morphology of the Z306 sample was clearly altered, as indicated by the SEM photographs in Figure 15. The flight sample has what appears to be a pitted or cratered surface, where portions of the surface were eroded away. This effect is not uniform across the surface, resulting in fairly large craters or pits. In contrast, the control sample has a fairly uniform texture, evenly distributed over the entire surface. The reasons for this erosion behavior are not understood.

The FTIR spectra for this sample as shown in Figure 16 do not indicate any significant chemical changes in the sample due to the atomic oxygen exposure.

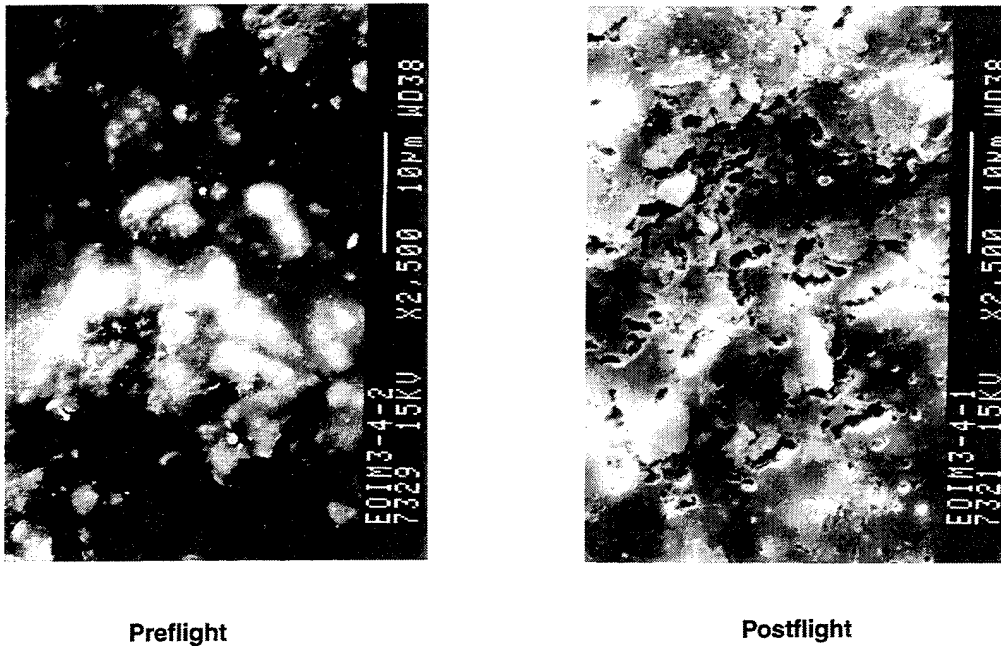


Figure 15. SEM photographs of EOIM3-4-1, Z306 LDEF TE (contaminated), before (left) and after (right) atomic oxygen exposure.

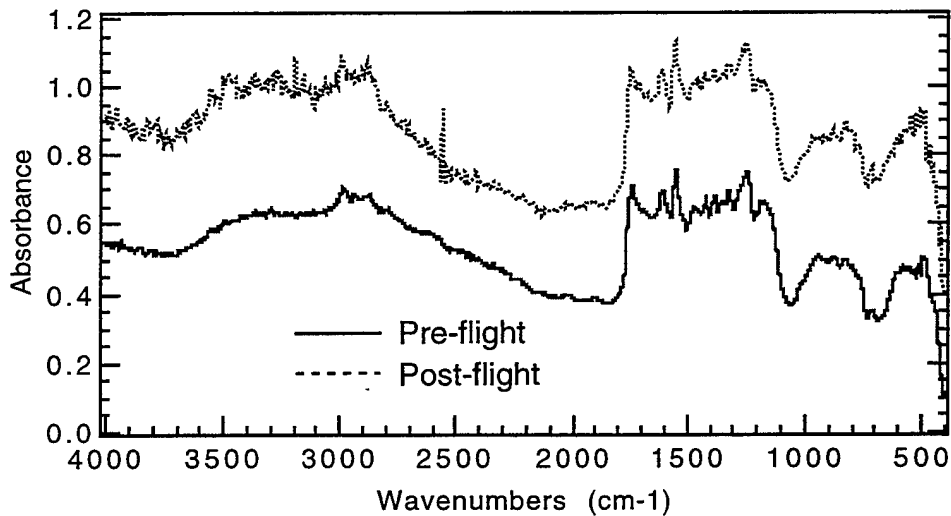


Figure 16. FTIR spectra of EOIM3-4-1, Z306 LDEF TE (contaminated), before and after atomic oxygen exposure.

The Z306 sample experienced weight loss due to the EOIM-III exposure (Table 1). This weight loss is consistent with the erosion of the surface; however, the magnitude of this erosion appears more significant than indicated by the sample weight change. Some of this erosion could have been offset by a weight gain due to contamination during the flight exposure.

### 5.5 Anodized Aluminum (TE, contaminated)

The anodized aluminum sample from the trailing edge of LDEF with a visible contamination layer is shown in Figure 17, post-flight. The sample exhibited an increase in its reflectance post-flight (Figure 18), resulting in a decrease in its solar absorptance from 0.394 to 0.330 (Table 2). The preflight XPS analysis indicated that the sample was contaminated with a layer of silica and silicones/silicates based on the Si2p peak.

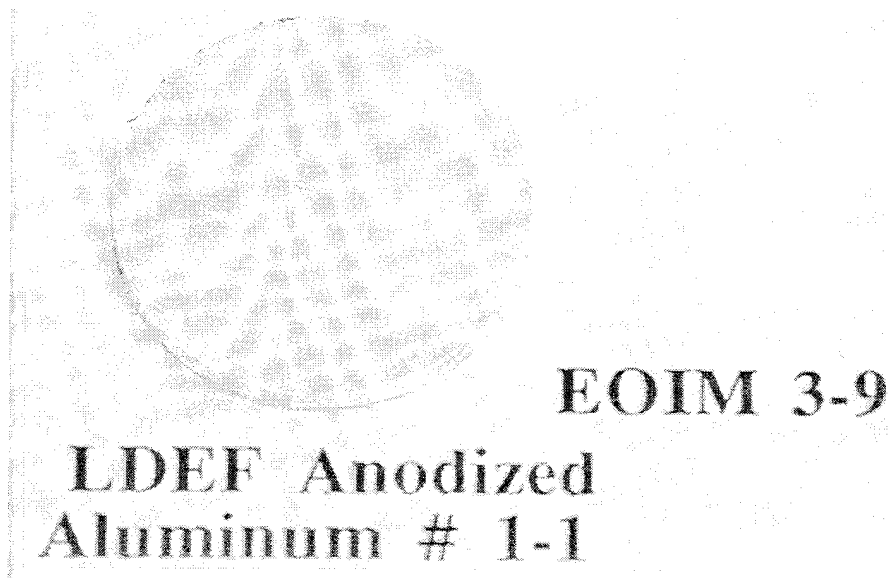


Figure 17. Post-flight photo of EOIM3-5-1, anodized aluminum LDEF TE (contaminated).

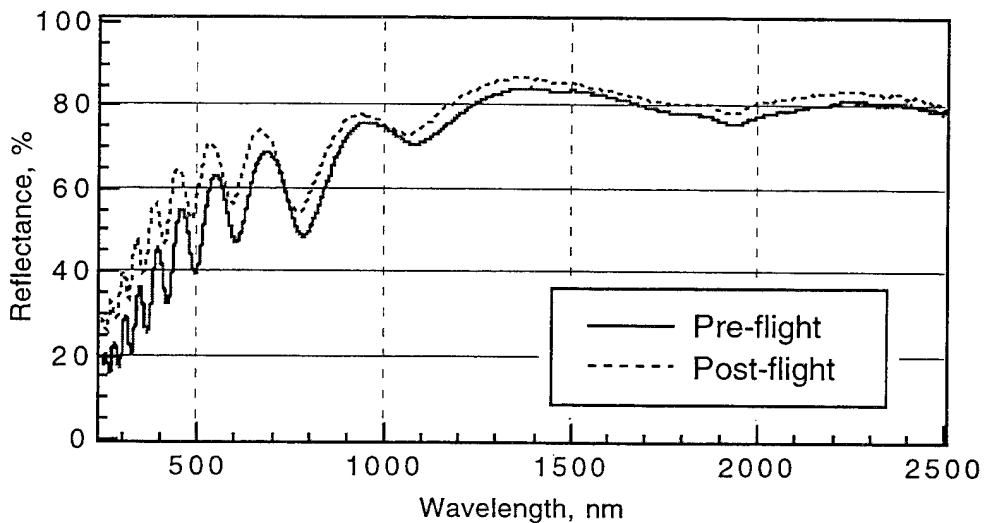


Figure 18. Reflectance spectra of EOIM3-5-1, anodized aluminum LDEF TE (contaminated), before and after atomic oxygen exposure.

Post-flight surface analysis showed additional surface deposition of silicon, increased surface oxidation, and decreased surface carbon concentration. The silicon concentration increased by 5 atom %, with new contaminant deposition. The decreased carbon signal, combined with the increased aluminum substrate signal, indicates that a significant portion of the carbon in the contaminant layer was removed by atomic oxygen during the flight. The increased silicon signal gives the most reliable data of the five samples, indicating that contamination occurred during the EOIM-III mission. The FTIR spectra shown in Figure 19 indicate that the contaminant layer has probably been thinned due to the exposure. Even with the silicon contamination, the sample still lost weight, as indicated in Table 1.

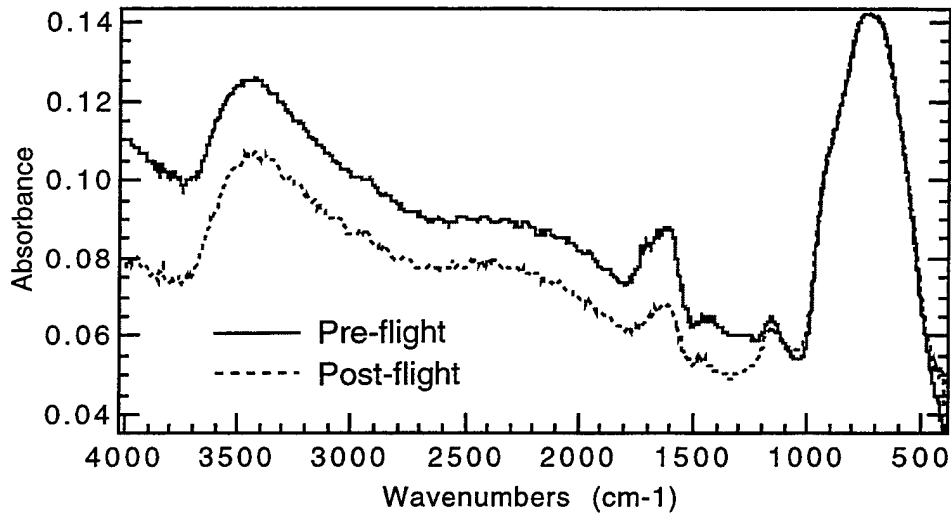


Figure 19. FTIR spectra of EOIM3-5-1, anodized aluminum LDEF TE (contaminated), before and after atomic oxygen exposure.

## 6. Comparison to Ground-Based Experiments

For comparison to the EOIM-III results, two LDEF samples of Chemglaze A276 (TE) and S13GLO (TE) similar to the samples flown on EOIM-III were exposed in the Hyperthermal Atomic Oxygen Facility at Los Alamos National Laboratory (LANL). These samples were cut from the same areas as the EOIM-III specimens.

The atomic oxygen facility at LANL consists of a continuous-wave laser sustained discharge source producing O-atoms having a variable energy of 1 to 5 eV at a flux of  $10^{16}$  to  $10^{17}$  atoms/cm<sup>2</sup>-s. A detailed description of the facility, including flux calculations, has been published.<sup>14,15</sup> In this experiment, exposures were made using a 50% Ar/50% O<sub>2</sub> gas mixture, with an estimated dissociation of O<sub>2</sub> of 95%. The kinetic energy of the atoms was 2 eV with a full-width-half maximum on the energy distribution curve of 1.5 eV. The total atomic oxygen exposure for the samples was  $2.0 \times 10^{20}$  atoms/cm<sup>2</sup> for Chemglaze A276 and  $1.6 \times 10^{20}$  atoms/cm<sup>2</sup> for S13GLO, which were similar to the total sample exposures on EOIM-III.

### 6.1 Chemglaze A276 (TE)

The LANL Chemglaze A276 sample showed similar effects to the EOIM-III flight sample. Visually, the sample changed from brown to white, as evidenced by the increased reflectance below 1500 nm (Figure 20) and the decreased solar absorptance from 0.536 to 0.258 (Table 2). In comparison with the reflectance data obtained from EOIM-III on the same material, the LANL paint sample exhibited greater increased reflectance post-test than the flight sample. Since both samples received the same atomic oxygen dose, the reasons for this are not clear.

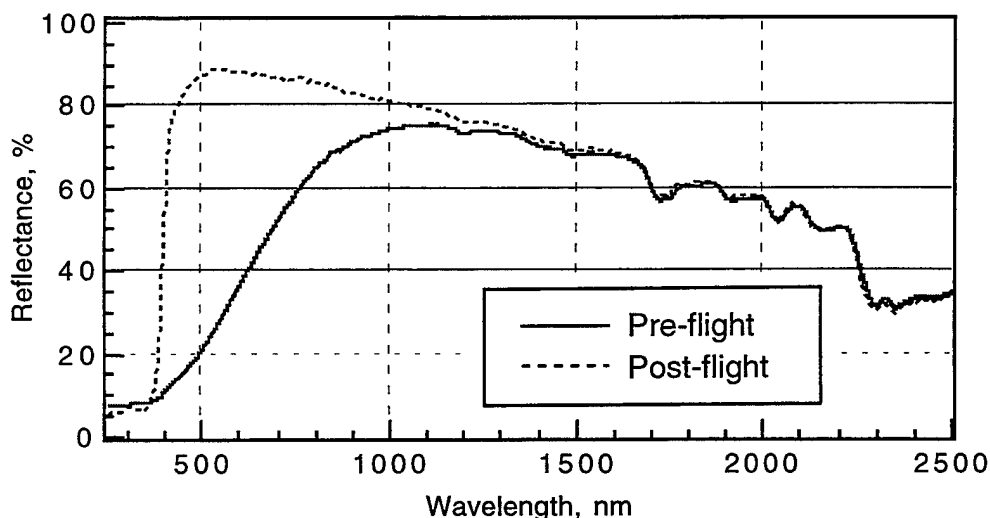
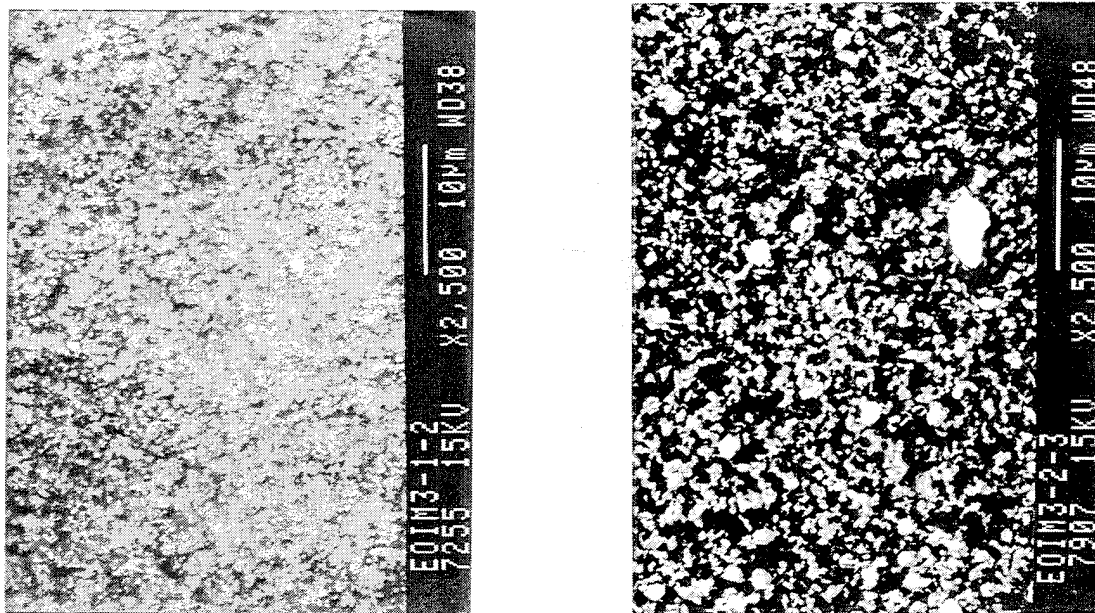


Figure 20. Reflectance spectra of EOIM3-1-3, Chemglaze A276 LDEF TE, before and after atomic oxygen exposure at LANL.

Atomic oxygen erosion of the polyurethane binder accounts for the changes in the surface morphology, as evident in the SEM photographs in Figure 21. Like the EOIM-III flight sample, exposure of the sample to atomic oxygen at LANL resulted in preferential erosion of the polyurethane binder, resulting in enrichment of titanium dioxide pigment at the surface.

The XPS data for the Chemglaze A276 sample is shown in Table 3. Comparable decreases in surface carbon concentration, about 40% relative, were noted after AO exposure at LANL and on EOIM-III. As discussed earlier, this loss of carbon is most likely due to the reaction of atomic oxygen with the polyurethane binder and surface contamination, creating volatile molecules that leave the surface. The surface silicon is probably due to surface contamination. However, some fraction of the relative increase in the surface silicon concentration could be due to the loss of surface carbon or to the aluminum silicate filler that is present in the chemglaze paints. Both the EOIM-III sample and the LANL sample experienced similar increases in the silicon concentrations. Based on the Si2p binding energy, the predominant state of silicon appears to be silica.<sup>11</sup> Similar to the EOIM-III sample, an increase in aluminum concentration is observed, which is attributed to the aluminum silicate filler. Importantly, no cracking or delaminations were seen in either the LANL or EOIM-III sample. Thus, the aluminum signal is not due to the paint substrate.



**Preflight**

**Postflight**

Figure 21. SEM photographs of EOIM3-1-3, Chemglaze A276 LDEF TE, before (left) and after (right) atomic oxygen exposure at LANL.

## 6.2 S13GLO (TE)

The S13GLO TE sample lightened during the ground-based atomic oxygen exposure at LANL, but visually it did not lighten as much as the EOIM-III flight sample. However, the change in the reflectance curve (Figure 22) is similar to the change observed for the flight sample (Figure 6). The change in solar absorptance from 0.422 to 0.386 is a little over half that observed for the flight sample (Table 2).

Investigation of the surface morphology with SEM (Figure 23) shows slight changes due to atomic-oxygen exposure. These changes are minor and, again, qualitatively less than observed for the EOIM-III sample.

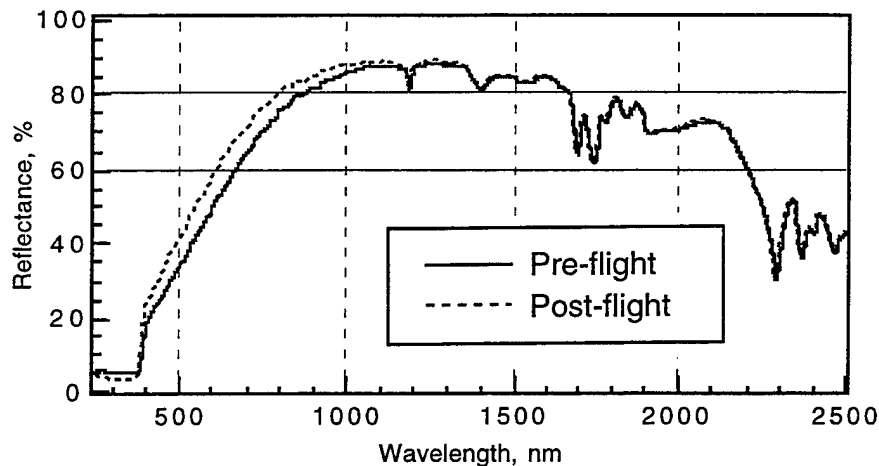


Figure 22. Reflectance spectra of EOIM3-2-3, S13GLO LDEF TE, before and after atomic oxygen exposure at LANL.

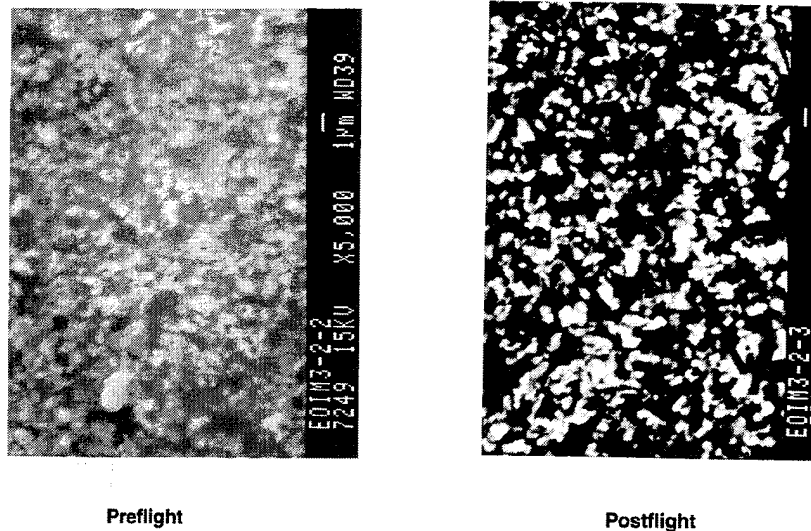


Figure 23. SEM photographs of EOIM3-2-3, S13GLO LDEF TE, before (left) and after (right) atomic oxygen exposure at LANL.

The pre-exposure XPS analysis of the LANL sample indicated surface composition similar to the EOIM-III flight sample (Table 3). Post-experiment analyses of the LANL AO experiment sample and the EOIM-III flight sample showed similar decreases in surface carbon concentration, increases in surface silicon concentration, and increases in surface oxygen. The decrease in surface carbon concentration of 30% relative is due to the loss of volatile molecules formed by atomic oxygen reactions, and also accounts for much of the relative increases in surface silicon and oxygen concentrations. The Si2p binding energy indicates that the predominant state on both surfaces is SiO<sub>2</sub>. Additionally, a shift in the charge-corrected binding energy of this peak of about half a volt indicates that some additional oxidation of residual surface silicones or silicates probably occurred during LANL AO exposure.<sup>11</sup>

Increases in surface potassium and zinc only occurred on the EOIM-III sample, indicating that the LANL AO experiment sample did not experience a significant loss of surface binder. In contrast, the EOIM-III sample showed an increase in potassium and a large increase in zinc, indicating that some loss of binder did occur. This difference may be caused by differences in thermal cycling and VUV exposure between the two AO exposure environments. Additionally, the EOIM-III sample was exposed to a 25% greater fluence than the ground-based LANL AO exposure sample, which could directly affect the amount of binder removed from the surface. AO exposure at LANL also resulted in a 60% relative decrease in surface nitrogen, while no decrease was noted for the EOIM-III sample. This discrepancy may indicate that nitrogen-containing contaminant deposition occurred on EOIM-III, balancing nitrogen loss due to AO reactions.<sup>11</sup>

## 7. Summary

The results from EOIM-III are consistent with the results and conclusions from LDEF. Several generalizations can be made:

- Exposure of retrieved TE LDEF paints to atomic oxygen either in ground-based facilities or on Shuttle sorties approximates LE phenomena observed on LDEF.
- While quite similar results were obtained between EOIM-III and LANL exposure studies, there are some small differences in the response of the paints to these two environments.
- Organic paint binders such as methyl silicone or polyurethane react with atomic oxygen to form volatile, carbon-based molecules that are removed from the paint surface.
- The methyl silicone binder in S13GLO, although still susceptible to reaction with atomic oxygen, is not as reactive as the Chemglaze A276 polyurethane binder.
- Depending on the chemical composition of the paint binder, erosion can occur that results in the exposure of pigment particles, which can affect the solar absorptance of the paint surface.
- The polyurethane binder in Chemglaze A276 degrades upon exposure to UV radiation, resulting in a significant increase in solar absorptance. Exposure of this surface to atomic oxygen results in erosion of the binder surface layers, resulting in enrichment of titanium dioxide pigment at the surface and a significant decrease in solar absorptance.
- Silicones and/or silicates tend to be oxidized by atomic oxygen to form silica,  $\text{SiO}_2$ . Erosion of the silicone occurs at the methyl groups, leading to a silicate and, eventually, silica.
- Not all surfaces are susceptible to atomic oxygen erosion, as displayed by the contamination layer on the S13GLO LE sample.
- Contaminated surfaces containing silicones that have been oxidized to silicates or silica are resistant to further erosion.

## References

1. Meshishnek, M. J., Gyetvay, S. R., and Jagers, C. H., "Long Duration Exposure Facility Experiment M0003 Deintegration/Findings and Impacts," LDEF—69 Months in Space, First Post-Retrieval Symposium, NASA Conference Publication 3134, pp. 1073–1108 (1991).
2. Golden, J. L., "Results of the Examination of the A276 White and Z306 Black Thermal Control Paint Disks Flown on LDEF," LDEF—69 Months in Space, First Post-Retrieval Symposium, NASA Conference Publication 3134, pp. 975–987 (1991).
3. Jagers, C. H., Coggi, J. M., and Meshishnek, M. J., "Thermal Control Paints on LDEF: Results of M0003 Sub-Experiment 18," LDEF—69 Months in Space, Second LDEF Post-Retrieval Symposium, NASA Conference Publication 3194, pp. 1075–1092 (1993).
4. Crutcher, E. R. and Warner, E. J., "Molecular Films Associated with LDEF," LDEF—69 Months in Space, First Post-Retrieval Symposium, NASA Conference Publication 3134, pp. 155–177 (1991).
5. Harvey, G. A., "Organic Contamination on LDEF," LDEF—69 Months in Space, First Post-Retrieval Symposium, NASA Conference Publication 3134, pp. 179–196 (1991).
6. Banks, B. A., Dever, J. A., Gebauer, L., and Hill, C. M., "Atomic Oxygen Interactions with FEP Teflon and Silicones on LDEF," LDEF—69 Months in Space, First Post-Retrieval Symposium, NASA Conference Publication 3134, pp. 801–815 (1991).
7. Pippin, G. and Crutcher, R., "Contamination of LDEF: Sources, Distribution and History," LDEF—69 Months in Space, Second LDEF Post-Retrieval Symposium, NASA Conference Publication 3194, pp. 1023–1033 (1993).
8. Blakkolb, B. K., Ryan, L.E., Bowen, H. S., and Kasic, T. J., "Optical Characterization of LDEF Contaminant Film," LDEF—69 Months in Space, Second LDEF Post-Retrieval Symposium, NASA Conference Publication 3194, pp. 1035–1040 (1993).
9. Stein, B. A., "LDEF Materials: An Overview of the Interim Findings," LDEF Materials Workshop '91, NASA Conference Publication 3162, pp. 1–56 (1991).
10. Stein, B. A., "LDEF Materials Overview," LDEF—69 Months in Space, Second LDEF Post-Retrieval Symposium, NASA Conference Publication 3194, pp. 741–789 (1993).
11. Hemminger, C.S., "XPS Analysis of Paint Samples Exposed to Atomic Oxygen at Los Alamos National Laboratory," ATM-93(3068)-1, 10 March 1993, The Aerospace Corporation.
12. Hemminger, C.S., "Surface Changes Measured by XPS on Select Samples Exposed to the Space Environment on EOIM-3," ATM- 92(2935-15)-8, 24 September 1992, The Aerospace Corporation.

13. Meshishnek, M. J., Stuckey, W. K., Evangelides, J. S., Feldman, L. A., and Peterson, R. V., "Effects on Advanced Materials: Results of the STS-8 EOIM Experiment," NASA Technical Memorandum 100459, Atomic Oxygen Effects For Shuttle Missions STS-8 and 41-G., Volume II, September 1988.
14. Cross, J. B., Spangler, L. H., Hoffbauer, M. A., and Archuleta, F. A., "High Intensity 5 eV cw Laser Sustained O-atom Exposure Facility for Material Degradation Studies," SAMPE Quarterly 18, 41 (1987).
15. Cross, J. B. and Blais, N. C., "High Energy/Intensity Atomic Oxygen Beam Source for Low Earth Orbit Materials Degradation Studies," Proceedings of the Sixteenth International Symposium on Rarefied Gas Dynamics, Pasadena, CA (1988).

## TECHNOLOGY OPERATIONS

The Aerospace Corporation functions as an "architect-engineer" for national security programs, specializing in advanced military space systems. The Corporation's Technology Operations supports the effective and timely development and operation of national security systems through scientific research and the application of advanced technology. Vital to the success of the Corporation is the technical staff's wide-ranging expertise and its ability to stay abreast of new technological developments and program support issues associated with rapidly evolving space systems. Contributing capabilities are provided by these individual Technology Centers:

**Electronics Technology Center:** Microelectronics, solid-state device physics, VLSI reliability, compound semiconductors, radiation hardening, data storage technologies, infrared detector devices and testing; electro-optics, quantum electronics, solid-state lasers, optical propagation and communications; cw and pulsed chemical laser development, optical resonators, beam control, atmospheric propagation, and laser effects and countermeasures; atomic frequency standards, applied laser spectroscopy, laser chemistry, laser optoelectronics, phase conjugation and coherent imaging, solar cell physics, battery electrochemistry, battery testing and evaluation.

**Mechanics and Materials Technology Center:** Evaluation and characterization of new materials: metals, alloys, ceramics, polymers and their composites, and new forms of carbon; development and analysis of thin films and deposition techniques; nondestructive evaluation, component failure analysis and reliability; fracture mechanics and stress corrosion; development and evaluation of hardened components; analysis and evaluation of materials at cryogenic and elevated temperatures; launch vehicle and reentry fluid mechanics, heat transfer and flight dynamics; chemical and electric propulsion; spacecraft structural mechanics, spacecraft survivability and vulnerability assessment; contamination, thermal and structural control; high temperature thermomechanics, gas kinetics and radiation; lubrication and surface phenomena.

**Space and Environment Technology Center:** Magnetospheric, auroral and cosmic ray physics, wave-particle interactions, magnetospheric plasma waves; atmospheric and ionospheric physics, density and composition of the upper atmosphere, remote sensing using atmospheric radiation; solar physics, infrared astronomy, infrared signature analysis; effects of solar activity, magnetic storms and nuclear explosions on the earth's atmosphere, ionosphere and magnetosphere; effects of electromagnetic and particulate radiations on space systems; space instrumentation; propellant chemistry, chemical dynamics, environmental chemistry, trace detection; atmospheric chemical reactions, atmospheric optics, light scattering, state-specific chemical reactions and radiative signatures of missile plumes, and sensor out-of-field-of-view rejection.